Cosmological constraints on parameters of effective theory of Standard Model

Artur Semushin[a]

[a]National Research Nuclear University MEPhI,

E-mail: artur.semushin@cern.ch

Contents

1 Introduction

Standard Model (SM) is the modern theory of particles that was completed in 2012 after experimental observation [1, 2] and discovery of a Higgs boson predicted by P. Higgs in 1964 [3]. However, the SM can't be a completed theory of everything due to some its problems. For example, SM doesn't include gravity, dark matter, dark energy, the masses of neutrino, etc. Furthermore, there are a few another important issues such as hierarchy problem, large number of free parameters, strong CP-problem, etc. Therefore, it is necessary to expand the SM. One of modern ways for indirect searching for new physics is effective field theory (EFT) [4]. This model-independent phenomenology effectively adds to the theory new couplings which are not presented in the SM (i.e. beyond-the-SM or BSM couplings) and enhances couplings which are presented in the SM. Setting limits on the new coupling constants can help to find the right direction for the SM extension.

On the other hand, there is a standard cosmological model, or a theory of a Big Bang, which describes evolution of the Universe. This model also contains a few problems, some of it are the same as the SM problems. Thus, combining of the particle and cosmological studies can lead to discovery of new physics. This report shows a few possible ways for combining EFT, that often used in analysis of data of accelerator experiments, and cosmology. Some related issues like the density of relic neutrino are considered.

2 Effective field theory

2.1 Introduction and aQGC

Effective extension of the SM consists in the parameterization of the Lagrangian with the operators of higher dimensions with some coefficients:

$$\mathcal{L} = \mathcal{L}_{\text{SM}} + \sum_i \sum_n \frac{F_{i,n}}{\Lambda^n} \mathcal{O}_i^{n+4} = \mathcal{L}_{\text{SM}} + \sum_i \sum_n f_{i,n} \mathcal{O}_i^{n+4}. \tag{1}$$

In this equation $\mathcal{L}_{\text{SM}}$ is the SM Lagrangian, Λ is the new physics energy scale, $\mathcal{O}_i^{n+4}$ is the i-th operator of $n+4$ dimension, $F_{i,n}$ is the corresponding unobservable dimensionless coefficient, $f_{i,n} = F_{i,n}/\Lambda^n$ is the corresponding (Wilson's) observable coefficient which has dimension TeV^{-n}.

In this report anomalous quartic gauge couplings (aQGC) was considered. It is convenient to study this couplings with operators of eight dimensions which lead to genuine aQGC without the contribution of anomalous triple gauge couplings (aTGC) [5]. These operators are constructed from covariant derivative of the Higgs field

$$D_\mu \Phi = \left(\partial_\mu + ig \frac{\sigma_i}{2} W_\mu^i + ig' \frac{1}{2} B_\mu \right) \Phi, \tag{2}$$

$SU(2)_L$ field strength tensor

$$\hat{W}_{\mu\nu} = \frac{\sigma^i}{2} W_{\mu\nu}^i, \tag{3}$$

where

$$W_{\mu\nu}^i = \partial_\mu W_\nu^i - \partial_\nu W_\mu^i + g \varepsilon^{ijk} W_\mu^j W_\nu^k, \tag{4}$$

and $U(1)_Y$ field strength tensor

$$B_{\mu\nu} = \partial_\mu B_\nu - \partial_\nu B_\mu \tag{5}$$

and can be divided into three families. S-family operators contain just covariant derivatives of the Higgs field:

$$\begin{aligned} \mathcal{O}_{\text{S0}} &= \left[(D_\mu \Phi)^\dagger D_\nu \Phi \right] \left[(D^\mu \Phi)^\dagger D^\nu \Phi \right], \\ \mathcal{O}_{\text{S1}} &= \left[(D_\mu \Phi)^\dagger D^\mu \Phi \right] \left[(D_\nu \Phi)^\dagger D^\nu \Phi \right]. \end{aligned} \tag{6}$$

T-family operators contain just gauge field strength tensors:

$$
\begin{aligned}
\mathcal{O}_{\mathrm{T0}} &= \mathrm{Tr}\left[\hat{W}_{\mu\nu}\hat{W}^{\mu\nu}\right]\mathrm{Tr}\left[\hat{W}_{\alpha\beta}\hat{W}^{\alpha\beta}\right], \\
\mathcal{O}_{\mathrm{T1}} &= \mathrm{Tr}\left[\hat{W}_{\alpha\nu}\hat{W}^{\mu\beta}\right]\mathrm{Tr}\left[\hat{W}_{\mu\beta}\hat{W}^{\alpha\nu}\right], \\
\mathcal{O}_{\mathrm{T2}} &= \mathrm{Tr}\left[\hat{W}_{\alpha\mu}\hat{W}^{\mu\beta}\right]\mathrm{Tr}\left[\hat{W}_{\beta\nu}\hat{W}^{\nu\alpha}\right], \\
\mathcal{O}_{\mathrm{T5}} &= \mathrm{Tr}\left[\hat{W}_{\mu\nu}\hat{W}^{\mu\nu}\right]\left[B_{\alpha\beta}B^{\alpha\beta}\right], \\
\mathcal{O}_{\mathrm{T6}} &= \mathrm{Tr}\left[\hat{W}_{\alpha\nu}\hat{W}^{\mu\beta}\right]\left[B_{\mu\beta}B^{\alpha\nu}\right], \\
\mathcal{O}_{\mathrm{T7}} &= \mathrm{Tr}\left[\hat{W}_{\alpha\mu}\hat{W}^{\mu\beta}\right]\left[B_{\beta\nu}B^{\nu\alpha}\right], \\
\mathcal{O}_{\mathrm{T8}} &= \left[B_{\mu\nu}B^{\mu\nu}\right]\left[B_{\alpha\beta}B^{\alpha\beta}\right], \\
\mathcal{O}_{\mathrm{T9}} &= \left[B_{\alpha\mu}B^{\mu\beta}\right]\left[B_{\beta\nu}B^{\nu\alpha}\right].
\end{aligned}
\tag{7}
$$

Finally, M-family operators mix covariant derivatives of the Higgs field and gauge field strength tensors:

$$
\begin{aligned}
\mathcal{O}_{\mathrm{M0}} &= \mathrm{Tr}\left[\hat{W}_{\mu\nu}\hat{W}^{\mu\nu}\right]\left[\left(D_\beta\Phi\right)^\dagger D^\beta\Phi\right], \\
\mathcal{O}_{\mathrm{M1}} &= \mathrm{Tr}\left[\hat{W}_{\mu\nu}\hat{W}^{\nu\beta}\right]\left[\left(D_\beta\Phi\right)^\dagger D^\mu\Phi\right], \\
\mathcal{O}_{\mathrm{M2}} &= \left[B_{\mu\nu}B^{\mu\nu}\right]\left[\left(D_\beta\Phi\right)^\dagger D^\beta\Phi\right], \\
\mathcal{O}_{\mathrm{M3}} &= \left[B_{\mu\nu}B^{\nu\beta}\right]\left[\left(D_\beta\Phi\right)^\dagger D^\mu\Phi\right], \\
\mathcal{O}_{\mathrm{M4}} &= \left[\left(D_\mu\Phi\right)^\dagger \hat{W}_{\beta\nu}D^\mu\Phi\right]B^{\beta\nu}, \\
\mathcal{O}_{\mathrm{M5}} &= \left[\left(D_\mu\Phi\right)^\dagger \hat{W}_{\beta\nu}D^\nu\Phi\right]B^{\beta\mu} + \mathrm{h.c.}, \\
\mathcal{O}_{\mathrm{M7}} &= \left[\left(D_\mu\Phi\right)^\dagger \hat{W}_{\beta\nu}\hat{W}^{\beta\mu}D^\nu\Phi\right].
\end{aligned}
\tag{8}
$$

From all possible quartic gauge couplings SM predicts just $WWWW$, $WWZZ$, $WWZ\gamma$, $WW\gamma\gamma$. Table 1 shows which quartic gauge couplings are affected by each operator.

Table 1: Influence of the 8-dimensional operators on quartic gauge couplings. Affected couplings are marked with a symbol ∘.

Operator	$WWWW$	$WWZZ$	$WWZ\gamma$	$WW\gamma\gamma$	$ZZZZ$	$ZZZ\gamma$	$ZZ\gamma\gamma$	$Z\gamma\gamma\gamma$	$\gamma\gamma\gamma\gamma$
$\mathcal{O}_{S0}$, $\mathcal{O}_{S1}$	∘	∘			∘				
$\mathcal{O}_{T0}$, $\mathcal{O}_{T1}$, $\mathcal{O}_{T2}$	∘	∘	∘	∘	∘	∘	∘	∘	∘
$\mathcal{O}_{T5}$, $\mathcal{O}_{T6}$, $\mathcal{O}_{T7}$		∘	∘	∘	∘	∘	∘	∘	∘
$\mathcal{O}_{T8}$, $\mathcal{O}_{T9}$					∘	∘	∘	∘	∘
$\mathcal{O}_{M0}$, $\mathcal{O}_{M1}$, $\mathcal{O}_{M7}$	∘	∘	∘	∘	∘	∘	∘		
$\mathcal{O}_{M2}$, $\mathcal{O}_{M3}$, $\mathcal{O}_{M4}$, $\mathcal{O}_{M5}$		∘	∘	∘	∘	∘	∘		

2.2 Amplitude decomposition

For studying processes using EFT one need to know how cross section depends on coefficient value. This dependence is considered in this section for the case when process contains not more that one new physics vertex.

In the general case, when Lagrangian is parameterized with a set of operators as

$$\mathcal{L} = \mathcal{L}_{\text{SM}} + \sum_i f_i \mathcal{O}_i, \tag{9}$$

amplitude of some process contains SM and beyond-the-SM (BSM) terms and can be written as

$$\mathcal{A} = \mathcal{A}_{\text{SM}} + \sum_i f_i \mathcal{A}_{\text{BSM},i}. \tag{10}$$

Square of this amplitude is

$$|\mathcal{A}|^2 = |\mathcal{A}_{\text{SM}}|^2 + \sum_i f_i 2\text{Re}(\mathcal{A}^\dagger_{\text{SM}} \mathcal{A}_{\text{BSM},i}) + \sum_i f_i^2 |\mathcal{A}_{\text{BSM},i}|^2 + \sum_{i,j,i>j} f_i f_j 2\text{Re}(\mathcal{A}^\dagger_{\text{BSM},i} \mathcal{A}_{\text{BSM},j}). \tag{11}$$

So, squared amplitude as well as cross section contains SM term, interference (linear) terms $\propto f_i$, quadratic terms $\propto f_i^2$ and cross terms $\propto f_i f_j$.

For setting 1D limits the Lagrangian is parameterized by a single operator as

$$\mathcal{L} = \mathcal{L}_{\text{SM}} + f\mathcal{O}. \tag{12}$$

In this case amplitude and its square are

$$\mathcal{A} = \mathcal{A}_{\text{SM}} + f\mathcal{A}_{\text{BSM}} \tag{13}$$

and

$$|\mathcal{A}|^2 = |\mathcal{A}_{\text{SM}}|^2 + f 2\text{Re}(\mathcal{A}^\dagger_{\text{SM}} \mathcal{A}_{\text{BSM}}) + f^2 |\mathcal{A}_{\text{BSM}}|^2. \tag{14}$$

Therefore, cross section contains one SM term, one interference term and one quadratic term and can be written as

$$\sigma = \sigma_{\text{SM}} + f\sigma_{\text{int}} + f^2 \sigma_{\text{quad}}. \tag{15}$$

If considered process is not predicted by the SM, then $\mathcal{A}_{\text{SM}} = 0$ and cross section is

$$\sigma = f^2 \sigma_{\text{quad}}. \tag{16}$$

3 Relic neutrino number density

3.1 Big Bang theory prediction

Number density of the relic neutrino is important for modern physics because it can help to test standard cosmological Big Bang model and models of BSM physics. However its observation is very difficult. Using Big Bang theory of early Universe, number density of the relic neutrino can be predicted [6].

Effective number of relativistic degrees of freedom is

$$g_* = \sum_{\text{bosons}} g_b + \frac{7}{8} \sum_{\text{fermions}} g_f. \tag{17}$$

The factor of 7/8 in the fermion term appears because bosons and fermions are followed to different statistic (Bose-Einstein and Fermi-Dirac ones respectively). After the uncoupling of the neutrino $g_*^1 = 11/2$ (photons, electrons and positrons contribute). After the e^+e^--annihilation only photons are relativistic and contribute, so $g_*^2 = 2$. Therefore, taking into account entropy conservation, one can find ratio of the CMB and neutrino temperatures which is constant after the e^+e^--annihilation:

$$\frac{T_\nu}{T_\gamma} = \left(\frac{g_*^2}{g_*^1}\right)^{1/3} = \left(\frac{4}{11}\right)^{1/3}. \tag{18}$$

Finally, taking into account that $n \propto T^3$, 3 flavours of neutrino and that number densities of relativistic fermions and bosons are related via a factor of 3/4 which has the same nature as a factor of 7/8 in Eq. 17, neutrino number density can be found as

$$n_\nu^0 = 3 \cdot \frac{3}{4} \cdot \frac{T_\nu^0}{T_0} n_\gamma^0 = \frac{9}{11} n_\gamma^0 \approx 336 \text{ cm}^{-3}. \tag{19}$$

3.2 Experimental limitations

There was not observations of relic neutrino to the moment. However direct experimental constraint on the number density of relic neutrino exists [7]:

$$\eta = \frac{n_\nu^{0,\text{observed}}}{n_\nu^0} \leq 7 \cdot 10^{11} \text{ (99\% CL)}. \tag{20}$$

Plot that illustrate this limit can be found in Fig. 1.

This limit is too large for using in physical estimations. There is an indirect way to constrain relic neutrino number density. Assuming that all what is not cold dark matter, baryons or dark energy is relic neutrino, one can write

$$\Omega_\nu = 1 - \Omega_c - \Omega_b - \Omega_\Lambda = 1 - \Omega_m - \Omega_\Lambda = 1 - (0.315 \pm 0.007) - (0.685 \pm 0.007) = 0 \pm 0.01. \tag{21}$$

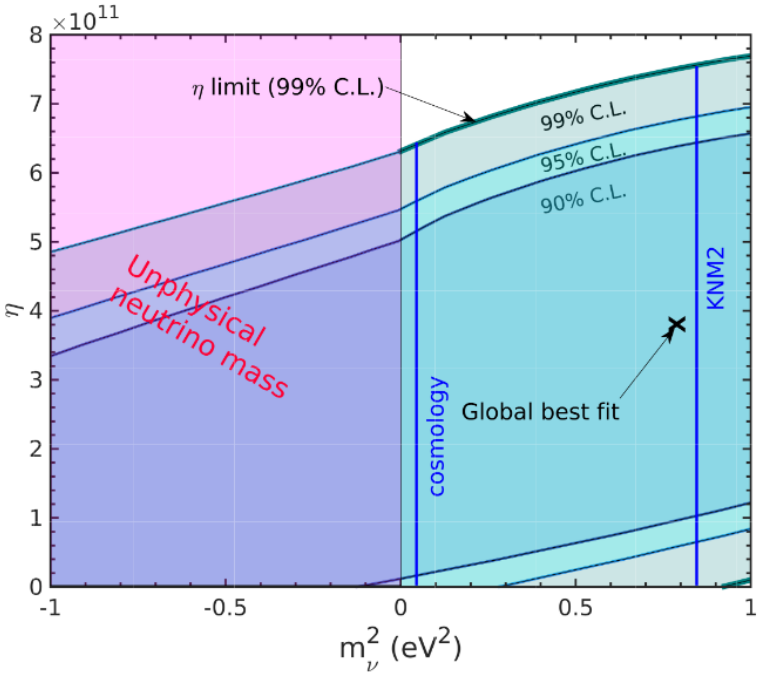

Figure 1: Limit on the number density of the relic neutrino.

Taking into account that Ω_ν is positive variable, approximately

$$\Omega_\nu < 0.02 \text{ (95\% CL)}. \tag{22}$$

Thus, observed relic neutrino number density can be written as

$$n_\nu^{0,\text{observed}} = \frac{\rho_\nu}{\sum m_\nu} = \frac{\Omega_\nu \rho_\text{crit}}{\sum m_\nu}. \tag{23}$$

Using limit $\sum m_\nu \geq 0.06$ eV obtained from mixing, one can find that

$$n_\nu^{0,\text{observed}} < 795 \text{ cm}^{-3}. \tag{24}$$

This limit is a few larger than Big Bang theory prediction and can be used for physical estimations.

4 Constraints from the CMB in the early Universe

4.1 Setting limits methodology

Such processes as $\gamma\gamma \to \nu\bar{\nu}\nu\bar{\nu}$ can affect modern relic neutrino number density [8], which expected and observed ones was estimated in Eq. 19 and 24 respectively. Of course, predicted neutrino number density from the anomalous couplings $n_\nu^{\text{pred},0}$ should be less than n_ν^0. Taking into account that predicted neutrino number density depends on EFT coupling constant f, condition

$$n_\nu^{\text{pred},0} < n_\nu^0 \tag{25}$$

can lead to constraint on f.

Neutrino number density from the anomalous couplings can be predicted as

$$n_\nu^{\text{pred},0} = \alpha_\nu n_0 = \frac{\alpha_\nu N_0}{V_0}, \tag{26}$$

where N_0 is the number of anomalous interactions that have occurred to present-day time moment, n_0 is N_0 per unit volume, α_ν is the number of neutrinos that are produced from a single anomalous interaction and V_0 is the present-day size of the Universe.

In the following calculations the first photon is incoming and the second photon is the mobile target. Assuming that CMB photons have Planck's energy distribution and isotropic spatial distribution, one can define the flux of the incoming photons

$$\frac{\mathrm{d}^4 N_1}{\mathrm{d}E_1\,\mathrm{d}\Omega_1\,\mathrm{d}S\,\mathrm{d}t} = f_{\text{Pl}}(E_1|T)\frac{1}{4\pi}n_\gamma c \tag{27}$$

and the distribution of the target photons

$$\frac{\mathrm{d}^2 N_2}{\mathrm{d}E_2\,\mathrm{d}\Omega_2} = f_{\text{Pl}}(E_2|T)\frac{1}{4\pi}n_\gamma V, \tag{28}$$

where T is the CMB temperature (Planck's distribution parameter), n_γ is CMB photons number density, c is the speed of light, V is the size of the Universe and

$$f_{\text{Pl}}(E|T) = \frac{qE^2}{e^{E/T}-1} \tag{29}$$

is the Planck's energy distribution normalized to unity with coefficient $q = (2\zeta(3)T^3)^{-1}$.

Since interacting photons have different energies and relative angle, it is necessary to know cross section dependence on this parameters. This can be done in the following way. Choosing spatial frame so that momentum of the first photon directed along the z axis, s invariant can be represented as

$$s = (p_1+p_2)^2 = 2(p_1p_2) = 2(E_1E_2 - \vec{p}_1\vec{p}_2) = 2E_1E_2(1-\cos\theta_2). \tag{30}$$

Then, obtaining cross section dependence on s invariant, one can obtain its dependence on E_1, E_2 and $\cos\theta_2$. Assuming that $\sigma(s)$ is a polynomial function

$$\sigma(s) = f^2 \sum_i p_i s^i \tag{31}$$

with $i > 0$ (anomalous cross section increases with energy), then

$$\sigma(E_1, E_2, \cos\theta_2) = f^2 \sum_i 2^i p_i E_1^i E_2^i (1 - \cos\theta_2)^i. \tag{32}$$

Frequency of the considered process is

$$\dot{N} = \int \sigma(E_1, E_2, \cos\theta_2) \frac{\mathrm{d}^4 N_1}{\mathrm{d}E_1\, \mathrm{d}\Omega_1\, \mathrm{d}S\, \mathrm{d}t} \frac{\mathrm{d}^2 N_2}{\mathrm{d}E_2\, \mathrm{d}\Omega_2}\, \mathrm{d}E_1\, \mathrm{d}E_2\, \mathrm{d}\Omega_1\, \mathrm{d}\Omega_2. \tag{33}$$

Taking into account Eq. 27, 28 and 32 and integrating over all angles θ_1, ϕ_1 and ϕ_2, it can be rewritten as

$$\dot{N} = \frac{1}{2} c n_\gamma^2 V f^2 \sum_i 2^i p_i \int E_1^i E_2^i (1 - \cos\theta_2)^i f_{\mathrm{Pl}}(E_1|T) f_{\mathrm{Pl}}(E_2|T)\, \mathrm{d}E_1\, \mathrm{d}E_2\, \mathrm{d}\cos\theta_2. \tag{34}$$

Integration by energy can be performed using formula

$$\int_0^\infty E^i f_{\mathrm{Pl}}(E|T)\, \mathrm{d}E = q \int_0^\infty \frac{E^{i+2}}{e^{E/T} - 1}\, \mathrm{d}E = q T^{i+3} \Gamma(i+3) \zeta(i+3), \tag{35}$$

where $\Gamma(x)$ is the gamma function and $\zeta(x)$ is Riemann zeta function. So the integral from Eq. 34 is

$$\begin{aligned}
&\int E_1^i E_2^i (1 - \cos\theta_2)^i f_{\mathrm{Pl}}(E_1|T) f_{\mathrm{Pl}}(E_2|T)\, \mathrm{d}E_1\, \mathrm{d}E_2\, \mathrm{d}\cos\theta_2 = \\
&\qquad = \int_0^\infty E_1^i f_{\mathrm{Pl}}(E_1|T)\, \mathrm{d}E_1 \int_0^\infty E_2^i f_{\mathrm{Pl}}(E_2|T)\, \mathrm{d}E_2 \int_{-1}^{1} (1 - \cos\theta_2)^i\, \mathrm{d}\cos\theta_2 = \\
&\qquad = \left(\int_0^\infty E^i f_{\mathrm{Pl}}(E|T)\, \mathrm{d}E \right)^2 \int_0^2 y^i\, \mathrm{d}y = q^2 T^{2i+6} \left(\Gamma(i+3)\zeta(i+3) \right)^2 \frac{2^{i+1}}{i+1} = \\
&\qquad\qquad = T^{2i} \frac{2^{i-1}}{i+1} \frac{\Gamma^2(i+3)\zeta^2(i+3)}{\zeta^2(3)},
\end{aligned} \tag{36}$$

where $y = 1 - \cos\theta_2$. Finally, frequency of the considered process can be rewritten as

$$\dot{N} = \frac{c n_\gamma^2 V f^2}{4\zeta^2(3)} \sum_i \frac{4^i}{i+1} p_i \Gamma^2(i+3) \zeta^2(i+3) T^{2i}. \tag{37}$$

In this formula CMB number density n_γ, CMB temperature T and size of the Universe V

depend on time t. In addition, anomalous interactions lead to a decrease in the CMB number density. So, n_γ depend on N. Therefore, Eq. 37 becomes a differential equation. Solving of this equation can be used for obtaining $n_\nu^{\text{pred},0}$ with Eq. 26 and setting limits with Eq. 25.

4.2 Choice of the time interval and dependencies estimation

Since in EFT cross sections increases with the energy, the most interesting stage of the Universe evolution for this study is radiation dominance stage (RD). Besides, non-zero mass of the neutrino leads to impossibility of reactions of neutrino production from CMB when energies of the photons are too small. Therefore, contribution from stages after RD is negligible. So upper time point can be chosen as $t_{\max} = 10^4$ yr. In the other side, neutrino had been in the equilibrium with another particles up to moment $t \approx 1$ s ($T \approx 1$ MeV). So lower time point can be chosen as $t_{\min} = 1$ s.

Number density from the CMB photons decreases due to the Universe expansion and from the anomalous interactions:

$$n_\gamma(t) = \left(n_\gamma^0 V_0 - \alpha_\gamma N(t)\right) \frac{1}{V(t)}, \tag{38}$$

where α_γ is the reducing of the number of CMB photons per single anomalous interaction. Thus Eq. 37 can be rewritten as

$$\frac{\mathrm{d}N}{\mathrm{d}t} = \left(n_\gamma^0 V_0 - \alpha_\gamma N\right)^2 \frac{1}{V(t)} \frac{cf^2}{4\zeta^2(3)} \sum_i \frac{4^i}{i+1} p_i \Gamma^2(i+3)\zeta^2(i+3) T^{2i}(t). \tag{39}$$

This is a differential equation, where variables N and t can be separated. After integrating by N from 0 to N_0 it can be seen that

$$\frac{1}{\alpha_\gamma}\left(\frac{1}{n_\gamma^0 V_0 - \alpha_\gamma N_0} - \frac{1}{n_\gamma^0 V_0}\right) = \int\limits_{t_{\min}}^{t_{\max}} \frac{1}{V(t)} \frac{cf^2}{4\zeta^2(3)} \sum_i \frac{4^i}{i+1} p_i \Gamma^2(i+3)\zeta^2(i+3) T^{2i}(t)\,\mathrm{d}t. \tag{40}$$

Multiplying this equation by $\alpha_\gamma V_0$ and taking into account that $V(t) \propto a^3(t)$ and $a(t) \propto T^{-1}(t)$, one can find that

$$\frac{1}{n_\gamma^0 - \alpha_\gamma n_0} - \frac{1}{n_\gamma^0} = \frac{\alpha_\gamma c f^2}{4\zeta^2(3) T_0^3} \sum_i \frac{4^i}{i+1} p_i \Gamma^2(i+3)\zeta^2(i+3) \int\limits_{t_{\min}}^{t_{\max}} T^{2i+3}(t)\,\mathrm{d}t \tag{41}$$

where $T_0 = 2.73$ K $= 2.35 \cdot 10^{-4}$ eV is observable present-day CMB temperature [9].

Dependence of the CMB temperature on time can be estimated from the facts that $T \propto a^{-1}$, $a \propto \sqrt{t}$ at the RD and condition that $T(t_{\min}) = T_{\min}$, where $T_{\min} = 1$ MeV. So, one can obtain

$$T(t) = T_{\min}\sqrt{\frac{t_{\min}}{t}}. \tag{42}$$

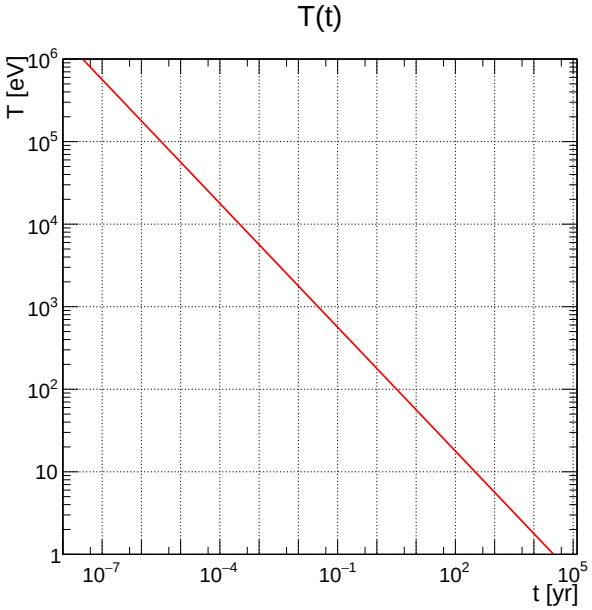

Figure 2: Dependence of the CMB temperature on time at the RD stage.

This dependence is shown in Fig. 2.

Integral from Eq. 41 denoted as I_i can be easily calculated as following:

$$I_i = \int_{t_{\min}}^{t_{\max}} T^{2i+3}(t)\,\mathrm{d}t = T_{\min}^{2i+3} t_{\min}^{i+3/2} \int_{t_{\min}}^{t_{\max}} \frac{\mathrm{d}t}{t^{i+3/2}} = \frac{T_{\min}^{2i+3} t_{\min}}{i+1/2}\left(1 - \left(\frac{t_{\min}}{t_{\max}}\right)^{i+1/2}\right). \tag{43}$$

Using Eq. 41, formula for n_0 can be written as

$$n_0 = \frac{n_\gamma^0}{\alpha_\gamma}\left(1 - \frac{1}{1 + f^2 \frac{\alpha_\gamma n_\gamma^0 c}{4\zeta^2(3)T_0^3} \sum_i \frac{4^i}{i+1} p_i \Gamma^2(i+3)\zeta^2(i+3) I_i}\right). \tag{44}$$

Then, using Eq. 25 and 26, constraint on f can be found as

$$|f| < \sqrt{\frac{1}{\alpha_\nu n_\gamma^0 - \alpha_\gamma n_\nu^0} \frac{n_\nu^0}{n_\gamma^0} \frac{4\zeta^2(3)T_0^3}{c \sum_i \frac{4^i}{i+1} p_i \Gamma^2(i+3)\zeta^2(i+3) I_i}}. \tag{45}$$

4.3 Cross section parameterization and results

Since in this work process $\gamma\gamma \to \nu\bar{\nu}\nu\bar{\nu}$ is considered, which diagram can be found in Fig. 3, one can set parameters defined in Eq. 26 and 38 as $\alpha_\nu = 4$ and $\alpha_\gamma = 2$.

For setting limits in this work coefficients of two operators of different families which affect $\gamma\gamma ZZ$ coupling were chosen: f_{T0} and f_{M0}. For cross section parameterization as in Eq. 31 Monte Carlo event generator MadGraph5 [10] was used. Table 2 shows cross section of considered process for different s. In Fig. 4 and Table 3 one can found fit of the dependence of cross section on s and its result. Finally, resulting limits on f_{T0} and f_{M0} can be found in Table 4.

For comparing, limits on some EFT coefficients observed by the CMS collaboration [11].

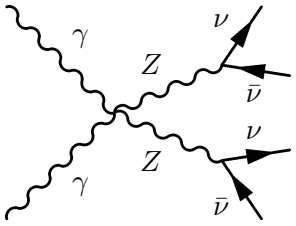

Figure 3: Diagram for process $\gamma\gamma \to \nu\bar{\nu}\nu\bar{\nu}$.

Table 2: Cross section for different s in case of one non-vanishing coefficient: f_{T0} (left) and f_{M0} (right). Coefficient value equals 1 TeV^{-4}.

s, GeV^2	$\sigma(f_{\mathrm{T0}} = 1\ \mathrm{GeV}^{-4})$, pb	$\sigma(f_{\mathrm{M0}} = 1\ \mathrm{GeV}^{-4})$, pb
$4 \cdot 10^{-8}$	$(6.13 \pm 0.08) \cdot 10^{-71}$	$(7.87 \pm 0.02) \cdot 10^{-48}$
10^{-6}	$(3.74 \pm 0.03) \cdot 10^{-61}$	$(7.70 \pm 0.02) \cdot 10^{-41}$
$4 \cdot 10^{-6}$	$(6.27 \pm 0.08) \cdot 10^{-57}$	$(7.87 \pm 0.04) \cdot 10^{-38}$
10^{-4}	$(3.73 \pm 0.01) \cdot 10^{-47}$	$(7.68 \pm 0.03) \cdot 10^{-31}$
$4 \cdot 10^{-4}$	$(6.18 \pm 0.02) \cdot 10^{-43}$	$(7.89 \pm 0.04) \cdot 10^{-28}$

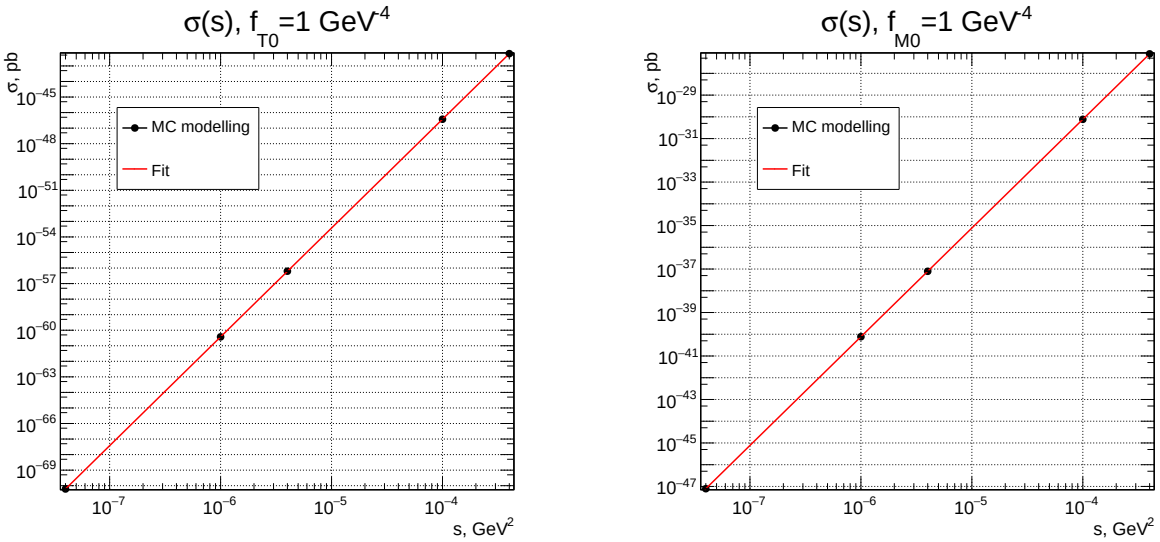

Figure 4: Fit of the cross section dependence on s with polynomial function 31 in case of one non-vanishing coefficient: f_{T0} (left) and f_{M0} (right). Coefficient value equals 1 TeV^{-4}.

Table 3: Resulting non-zero parameters of the fit described in Fig. 4.

Coefficient	Parameters
f_{T0}	$p_7 = 3.74 \cdot 10^{-19}$ pb/GeV^6
f_{M0}	$p_5 = 7.69 \cdot 10^{-11}$ pb/GeV^2

Table 4: Resulting limits on f_{T0} and f_{M0}.

Coefficient	Limit, TeV^{-4}
f_{T0}	$4.0 \cdot 10^{32}$
f_{M0}	$5.9 \cdot 10^{24}$

Taking into account results from Table 4, one can conclude, that the theory of a Big Bang is compatible with EFT extension of the SM, at least within considered model. Furthermore, this

technique can't lead to limits comparable with the results of the collider experiments due to low temperatures of the Universe in the considered time interval.

Table 5: Observed by the CMS collaboration [11] limits on some EFT coefficients.

Coefficient	f_{T0}	f_{T5}	f_{T8}	f_{M0}	f_{M1}
Limit on $\lvert f\rvert$, TeV^{-4}	0.64	0.64	0.47	16.0	35.0

5 Cosmological interpretation of the aQGC

5.1 Interpretation in terms of multicharged fermions

In this section possible interpretation of aQGC from 8-dimensional operators is considered by the example of the scattering of the photons. Diagram of this process predicted by the T-family EFT operators is presented in Fig. 5. EFT operators of M- and S- families don't predict this process on the tree level (Table 1).

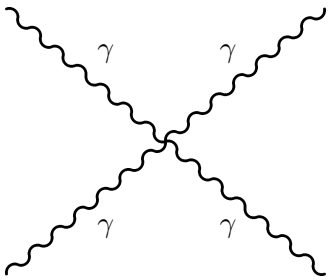

Figure 5: Diagram of the scattering $\gamma\gamma \to \gamma\gamma$ which predicted by T-family EFT operators.

In general case of some BSM scattering, cross section dependence on the energy ω of the initial particles in the center-of-mass system can be found from simple dimension analysis. Amplitude of the process in proportional to f, fv^2 and fv^4 for operators of T-, M- and S-family respectively. Therefore, to ensure the correct dimension of the cross-section, its dependence in the energy ω should be the following:

$$\begin{aligned} &\sigma \propto \omega^6, && \text{T-family}, \\ &\sigma \propto \omega^2, && \text{M-family}, \\ &\sigma \propto \omega^{-2}, && \text{S-family}. \end{aligned} \tag{46}$$

For $\gamma\gamma$-scattering this dependence was verified using Monte-Carlo simulations. Plots which illustrate this dependence for cases of f_{T0} and f_{T8} non-zero EFT coefficients can be found in Fig. 6. Fitting function for this plots was function $\sigma = f^2 p_3 \sigma^3$. Results of the fits can be found in Table 6. Taking into account that $s = 4\omega^2$, final dependence on ω for $\gamma\gamma$-scattering is

$$\sigma = f^2 \cdot 64 p_3 \omega^6. \tag{47}$$

Table 6: Results of the fit of the dependence of the cross section on the s-invariant for $\gamma\gamma$-scattering for cases of f_{T0} and f_{T8} non-zero EFT coefficients.

Coefficient	p_3, pb·TeV^2
f_{T0}	$9.69 \cdot 10^{-2}$
f_{T8}	$1.79 \cdot 10^{2}$

It can be seen that this dependence on the photon energy is the same as in case of low-energy $\gamma\gamma$-scattering through a fermionic loop. Example of the diagram of this process can be found

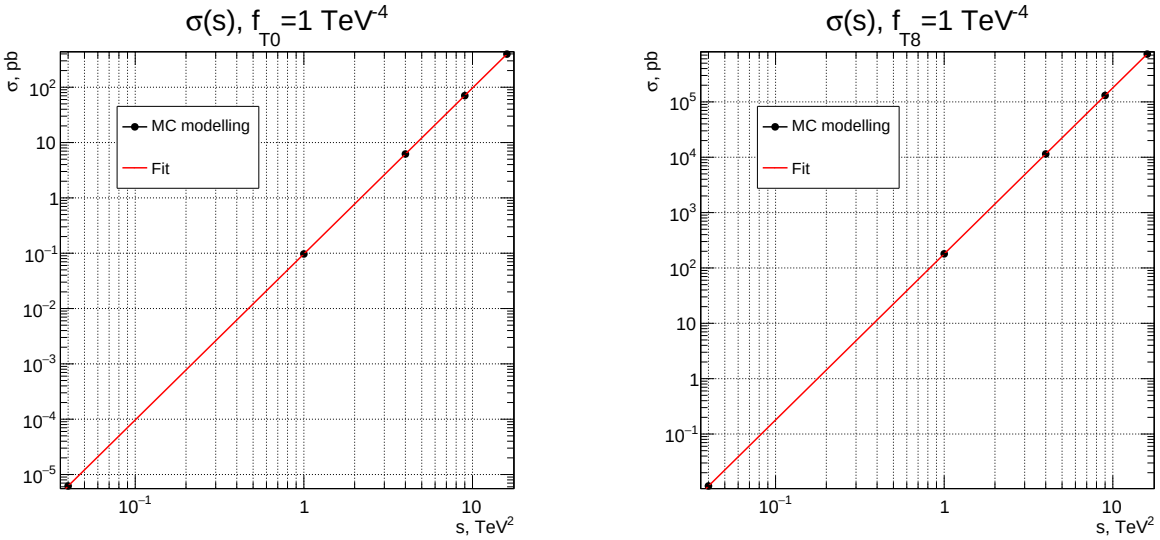

Figure 6: Dependence of the cross section on the s-invariant for $\gamma\gamma$-scattering for cases of f_{T0} (left) and f_{T8} (right) non-zero EFT coefficients.

in Fig. 7. If fermion in the loop is the electron, then low-energy ($\omega \ll m_e$) cross-section is [12]

$$\sigma = 0.031\alpha^2 r_e^2 \left(\frac{\omega}{m_e}\right)^6. \tag{48}$$

This result can be generalized to the case of heavy fermion with mass m and electric charge Z (in the units of e):

$$\sigma = 0.031 Z^8 \alpha^4 \frac{\omega^6}{m^8}. \tag{49}$$

It should be emphasized that EFT is valid when $\omega \ll \Lambda$, when Λ is the new physics energy scale (Eq. 1). In this case $\Lambda = m$, then only case $\omega \ll m$ can be considered.

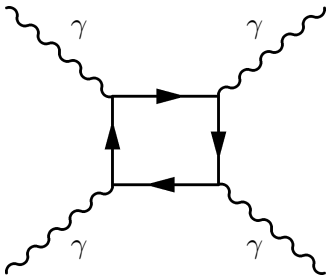

Figure 7: Example of the diagram for $\gamma\gamma$-scattering through a fermionic loop.

Following the interpretation of effective $\gamma\gamma$-scattering as scattering through a heavy fermion with a mass m and electric charge Z in the units of e, one can equate cross sections from Eq. 47 and 49:

$$0.031 Z^8 \alpha^4 \frac{\omega^6}{\Lambda^8} = f^2 \cdot 64 p_3 \omega^6. \tag{50}$$

It leads to a couple of physical results. First, interpreting Λ as m and taking into account that

$f = \dfrac{F}{\Lambda^4}$, one can find dimensionless EFT coupling constant:

$$F = \frac{0.031 Z^8 \alpha^4}{64 p_3}. \tag{51}$$

Using results from Table 6 it can be found that

$$\begin{aligned} F_{\mathrm{T0}} &\approx 7.0 \cdot 10^{-9} \cdot Z^8, \\ F_{\mathrm{T8}} &\approx 3.8 \cdot 10^{-12} \cdot Z^8. \end{aligned} \tag{52}$$

The second result is indirect limitation on the mass of the multicharged particles. Eq. 50 (with the replacement of Λ for m) can be rewritten as

$$m = |Z| \left(\frac{0.031 \alpha^4}{64 p_3 f^2} \right)^{1/8} = |Z| \left(\frac{F}{Q^8} \frac{1}{f^2} \right)^{1/8}. \tag{53}$$

Using Table 5 one can find indirect mass limitation:

$$\begin{aligned} m &> |Z| \cdot 0.11\mathrm{GeV} \text{ (from } f_{\mathrm{T0}}), \\ m &> |Z| \cdot 0.05\mathrm{GeV} \text{ (from } f_{\mathrm{T8}}). \end{aligned} \tag{54}$$

The observed by the ATLAS collaboration [13] mass limits on the multicharged particles in case of lepton-like particles can be found in Fig. 8. Direct experimental limits are more strict than indirect ones. However for large Z indirect limits can be tighter than direct ones.

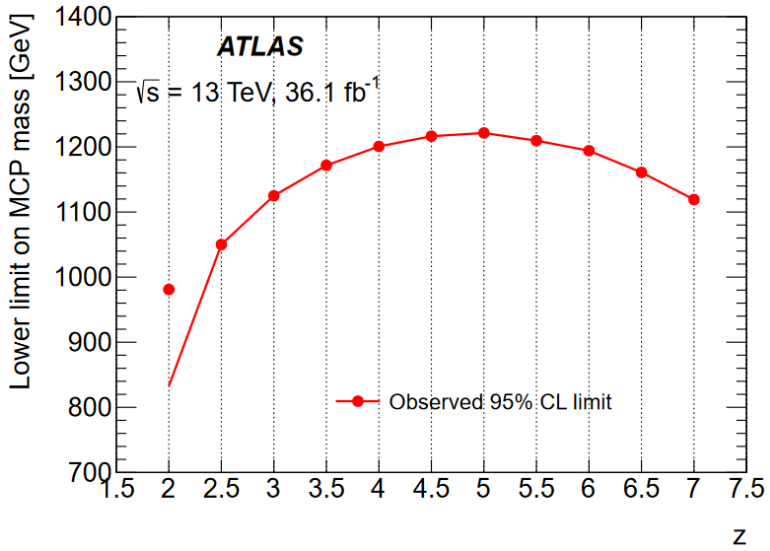

Figure 8: Limits on the multicharged particles (MCPs) masses observed by the ATLAS collaboration [13].

5.2 Cosmological model with fermions with $-2n$ charge

Since the dark matter (DM) [14] is not described by the SM, EFT should predict the manifestations of the DM. So the multicharged particles with large mass can be applied in this problem. An important for cosmology case is $Z = -2n$, where n is an natural number. These hypothetical lepton-like particles (X^{-2n}) in the early Universe can form atoms with He nuclei by ordinary Coulomb force. In the simplest case of $n = 1$ this particle is O^{-2} and corresponding atom is OHe. These atoms called dark atoms [15] are good candidates to the DM components [16].

Electric charge of $-2n$ of these particles is determined by the following considerations [17]. BSM particle with -1 charge after Big Bang nucleosynthesis should bind with primordial He forming ion with $+1$ charge which then capture an electron forming anomalous hydrogen atom. BSM particle with $+1$ charge also should form anomalous hydrogen nucleus with an electron. Concentration of the anomalous hydrogen in the terrestrial matter strictly constrained. Therefore, only BSM particles with $-2n$ electric charge can avoid this problem.

6 Conclusion

In this work some possible ways for applying of EFT methodology to cosmology were considered. The first way consists of setting limits on EFT coefficient from cosmological data. Anomalous process $\gamma\gamma \to \nu\bar{\nu}\nu\bar{\nu}$ was considered for setting limits on $f_{\mathrm{T}0}$ and $f_{\mathrm{M}0}$ coefficients. Resulting limits are much less stringent than limits from collider experiments. Consequently, the Big Bang theory is in agreement with the EFT extension of the SM, and this way is not perspective for searching for new physics within considered model. The second technique consists of setting limits on some properties of the hypothetical particles using observed limits on the EFT coefficients. For this purposes process $\gamma\gamma \to \gamma\gamma$ was considered. This anomalous process added in the theory with the operators of T-family can be interpreted as scattering of the photons through a loop with unknown fermions. From these considerations indirect limits on the mass of the unknown fermion can be set. Comparing this limits with the limits from direct experimental searches for multicharged particles, one can conclude that for low charges $|Z|$ indirect mass limit is a few less tight than direct one. However in case of high charges indirect limit becomes tighter than direct one due to the fact that indirect limit growth linearly with increasing of the $|Z|$. So, this way for searching for new physics is more perspective than the first one.

References

[1] ATLAS collaboration, *Observation of a new particle in the search for the Standard Model Higgs boson with the ATLAS detector at the LHC*, *Phys. Lett. B* **716** (2012) 1 [1207.7214].

[2] CMS collaboration, *Observation of a New Boson at a Mass of 125 GeV with the CMS Experiment at the LHC*, *Phys. Lett. B* **716** (2012) 30 [1207.7235].

[3] P.W. Higgs, *Broken symmetries, massless particlees and gauge fields*, *Physics Letters* **12** (1964) 132.

[4] C. Degrande, N. Greiner, W. Kilian, O. Mattelaer, H. Mebane, T. Stelzer et al., *Effective Field Theory: A Modern Approach to Anomalous Couplings*, *Annals Phys.* **335** (2013) 21 [1205.4231].

[5] O.J.P. Éboli and M.C. Gonzalez-Garcia, *Classifying the bosonic quartic couplings*, *Phys. Rev. D* **93** (2016) 093013 [1604.03555].

[6] D. Gorbunov and V. Rubakov, *Introduction to the theory of the early universe: Hot big bang theory*, World Scientific (01, 2011), 10.1142/7874.

[7] F. Kellerer, *First constraint on the relic neutrino background with KATRIN data*, Master's thesis, Technical University of Munich, 2021.

[8] Particle Data Group collaboration, *Review of Particle Physics*, *PTEP* **2020** (2020) 083C01.

[9] Planck collaboration, *Planck 2018 results. VI. Cosmological parameters*, *Astron. Astrophys.* **641** (2020) A6 [1807.06209].

[10] J. Alwall, R. Frederix, S. Frixione, V. Hirschi, F. Maltoni, O. Mattelaer et al., *The automated computation of tree-level and next-to-leading order differential cross sections, and their matching to parton shower simulations*, *JHEP* **07** (2014) 079 [1405.0301].

[11] CMS collaboration, *Measurement of the electroweak production of $Z\gamma$ and two jets in proton-proton collisions at $\sqrt{s} = 13$ TeV and constraints on anomalous quartic gauge couplings*, *Phys. Rev. D* **104** (2021) 072001 [2106.11082].

[12] V.B. Berestetskii, E.M. Lifshitz and L.P. Pitaevskii, *Quantum Electrodynamics*, vol. 4 of *Course of Theoretical Physics*, Butterworth-Heinemann, 2nd ed. (1982).

[13] ATLAS collaboration, *Search for heavy long-lived multicharged particles in proton-proton collisions at $\sqrt{s} = 13$ TeV using the ATLAS detector*, *Phys. Rev. D* **99** (2019) 052003 [1812.03673].

[14] M. Khlopov, *Cosmoparticle physics of dark matter*, *EPJ Web Conf.* **222** (2019) 01006 [1910.12910].

[15] M.Y. Khlopov, A.G. Mayorov and E.Y. Soldatov, *The dark atoms of dark matter*, *Prespace. J.* **1** (2010) 1403 [1012.0934].

[16] V.A. Gani, M.Y. Khlopov and D.N. Voskresensky, *Superheavy objects composed of nuclear and dark matter*, *J. Phys. Conf. Ser.* **1390** (2019) 012095 [1901.05930].

[17] D. Fargion and M. Khlopov, *Tera-leptons' shadows over Sinister Universe*, *Grav. Cosmol.* **19** (2013) 219 [hep-ph/0507087].